Applied Mathematical Modelling 46 (2017) 750–762

Contents lists available at ScienceDirect

Applied Mathematical Modelling

journal homepage: www.elsevier.com/locate/apm

Computational implementation of the rigid finite element method in the statics and dynamics analysis of forest cranes

Andrzej Urbaś*

University of Bielsko-Biala, Department of Mechanics, Willowa 2, 43-309 Bielsko-Biala, Poland

A R T I C L E I N F O

Article history:
Received 28 March 2016
Revised 2 July 2016
Accepted 3 August 2016
Available online 12 August 2016

Keywords:
Rigid finite element method
Forest crane
Statics analysis
Dynamics analysis

A B S T R A C T

A general mathematical model of a forest crane for statics and dynamics analysis is presented in the paper. This model allows to take into account the crane's flexible connections with the ground, the flexibility of its links and drives. The rigid finite element method is used to discretize the flexible links. Joint coordinates and homogeneous transformation matrices are used to describe the geometry of the system. Equations of motion are derived using the formalism of Lagrange equations. As an example, a forest crane built of eight links is presented. It is assumed that only one selected link of the crane is flexible. The influence of the flexibility of the link on the movements of load and driving torques in the revolute joints and the driving force in the prismatic joint are analyzed. The results may have practical significance, e.g. in terms of the selection of drives.

1. Introduction

The preparation stage of virtual prototypes is very import during the design process. Thanks to high computational capabilities, advanced mathematical models can now be prepared using commercial software or the author's programs developed to analyze new methods or phenomena. Therefore, a virtual prototype is tested in the design process which supports the constructor in building the real prototype with its specific requirements.

When mathematical models of cranes are prepared, they take into account different phenomena, e.g. the stability of the cranes, the strength of their links or stability of the load motion. Other phenomena are, e.g. the flexibility of the support system [1–11] or the flexibility of the load-bearing system (links [9,12–16], hoist rope [1,15,17]), drive system [9,18,19].

The general model of a forest crane [20–26] for statics and dynamics analysis is presented in the paper. The flexibility of the support system, links and drives is taken into account in this model. The rigid finite element method is used to discretize the flexible links [27,28]. This method depends on the division of the link into series of rigid elements interconnected by means of six spring-damping elements which model longitudinal, lateral, bending and torsional flexibility. The modified form of this method, which is reduced to take into account the bending and torsional flexibility of the links to a statics [29,30] and dynamics [31,32] analysis, is used in the paper. As a result of discretization of the links of the crane using the rigid finite element method, the system in the form of an open-loop kinematic chain is obtained. For this system, the classical methods of formulating equations dynamics can be used. In this model it is assumed that the rotating links of the cranes are driven directly by the driving torques, whereas the moving links are driven by driving forces. This is a simplification because in a real system the links are driven by hydraulic actuators (changing the jib crane and telescoping). The crane's model as

* Fax: +48 338279257.
E-mail addresses: aurbas@ath.bielsko.pl, aurbas@ath.eu

http://dx.doi.org/10.1016/j.apm.2016.08.006
0307-904X/

Nomenclature

g	acceleration of gravity
i	symbol of support
p	symbol of link (joint, drive)
rfe(p, i)	symbol of $i$thrigid finite element of link p
sde(p, i)	symbol of $i$thspring-damping element of link p
$e_{s,\alpha}^{(i)}\vert_{\alpha\in\{x,y,z\}}$	elongation of support i in α direction
$l^{(p)}$	length of link p
$l_{s,\alpha,0}^{(i)}, l_{s,\alpha}^{(i)}\vert_{\alpha\in\{x,y,z\}}$	initial and current length of support i in α direction
$m^{(p)}$	mass of link p
$\tilde{n}_{dof}^{(p)}$	number of generalized coordinates describing the motion of link p with respect to link $p-1$, $\tilde{n}_{dof}^{(p)} \le 6$
$n_{dof}^{(p)}$	number of generalized coordinates describing the motion of link p with respect to reference system {0}
$n_{div}^{(p)}$	number of division of link p
$n_{sde}^{(p)}$	number of sdes of link p
$n_{rfe}^{(p)}$	number of rfes of link p
n_{dr}	number of drives
n_f	number of flexible links
n_l	number of links
n_s	number of supports
$s_{s,\alpha}^{(i)}, d_{s,\alpha}^{(i)}\vert_{\alpha\in\{x,y,z\}}$	stiffness and damping coefficients of support i in α direction
$s_{l,\alpha}^{(p,i)}, d_{l,\alpha}^{(p,i)}\vert_{\alpha\in\{\psi,\theta,\varphi\}}$	stiffness and damping coefficients of rfe(p, i)
$s_{dr}^{(p)}, d_{dr}^{(p)}$	stiffness and damping coefficients of drive p
E_k	kinetic energy of the system
E_p	potential energy of the system
$E_{p,\,dr}$	potential energy of spring deformation of the drives
$E_{p,\,g}$	potential energy of gravity forces
$E_{p,\,l}$	potential energy of spring deformation of the links
$E_{p,\,s}$	potential energy of spring deformation of supports
R	Rayleigh dissipation function of the system
R_{dr}	Rayleigh dissipation function of the drives
R_l	Rayleigh dissipation function of the links
R_s	Rayleigh dissipation function of the supports
$I_{\hat{\mathbf{x}}^{(p)}}^{(p)},\ I_{\hat{\mathbf{y}}^{(p)}}^{(p)},\ I_{\hat{\mathbf{z}}^{(p)}}^{(p)}$	mass moments of inertia of link p
$I_{\hat{\mathbf{x}}^{(p)}\hat{\mathbf{y}}^{(p)}}^{(p)},\ I_{\hat{\mathbf{x}}^{(p)}\hat{\mathbf{z}}^{(p)}}^{(p)},\ I_{\hat{\mathbf{y}}^{(p)}\hat{\mathbf{z}}^{(p)}}^{(p)}$	mass products of inertia of link p
$I_{(\hat{\mathbf{y}}^{(p)}\hat{\mathbf{z}}^{(p)})}^{(p)},\ I_{(\hat{\mathbf{x}}^{(p)}\hat{\mathbf{z}}^{(p)})}^{(p)},\ I_{(\hat{\mathbf{x}}^{(p)}\hat{\mathbf{y}}^{(p)})}^{(p)}$	area moments of inertia of link p
$S_{\hat{\mathbf{x}}^{(p)}}^{(p)},\ S_{\hat{\mathbf{y}}^{(p)}}^{(p)},\ S_{\hat{\mathbf{z}}^{(p)}}^{(p)}$	static moments of link p
$\tilde{\mathbf{q}}^{(p)}$	vector of generalized coordinates describing the motion of link p with respect to link $p-1$, $\tilde{\mathbf{q}}^{(p)} = (\tilde{q}_j^{(p)})_{\substack{p=1,\ldots,n_l \\ j=1,\ldots,\tilde{n}_{dof}^{(p)}}}$
$\mathbf{q}^{(p)}$	vector of generalized coordinates describing the motion of link p with respect to reference system {0}, $\mathbf{q}^{(p)} = (q_j^{(p)})_{\substack{p=1,\ldots,n_l \\ j=1,\ldots,n_{dof}^{(p)}}}$
$\mathbf{r}_{C^{(p)}}^{(p)}$	vector of position of point $C^{(p)}$ defined in the local coordinate system of link p
$\mathbf{t}_{dr}^{(p)}$	driving torque (force) of link p
$\mathbf{H}^{(p)}$	pseudo-inertia matrix of link p
$\tilde{\mathbf{T}}^{(p)}$	homogeneous transformation matrix from the local coordinate system of link p to the system of link $p-1$
$\mathbf{T}^{(p)}$	homogeneous transformation matrix from the local coordinate system of link p to reference system {0}

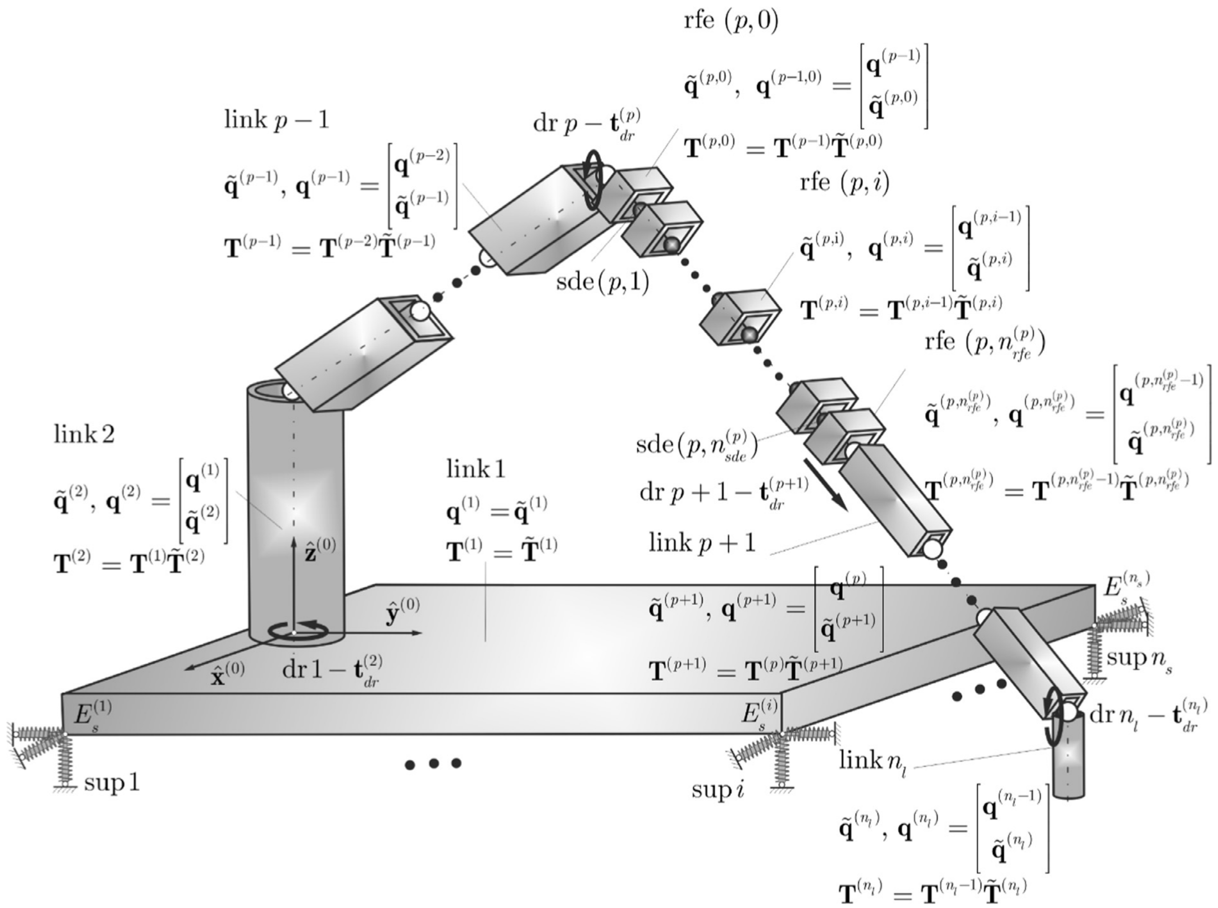

Fig. 1. General model of a forest crane.

assumed here has the structure of an open-loop kinematic chain. Therefore, the Denavit–Hartenberg notation [33], based on joint coordinates and homogeneous transformations matrices [34–36], can be used to describe the geometry of the cranes. Equations of the crane's motion are derived using the formalism of Lagrange equations and the algorithms presented in monograph [37], and also partly in monograph [38]. The numerical calculations include statics analysis (determining the initial configuration of the system as a result of taking into consideration the flexibility of the supports, links and drives) and dynamics analysis. The statics equations (nonlinear algebraic equations) are solved using the Newton–Raphson method. The dynamics equations (ordinary differential equations) are integrated by using the classical explicit Runge–Kutta method of the fourth order with a constant step size.

A model of a forest crane built with eight links is presented as an example of the mathematical model proposed here. It is assumed that only one selected link is flexible and five links have their own drives. The influence of the flexibility of the link on the trajectory of the selected points of the load and driving torques in the revolute joints and the driving force in the prismatic joint are analyzed.

2. General model of a forest crane

The general model of a forest crane built of n_l links (link $p|_{p=1,\ldots,n_l}$) is presented in Fig. 1. The crane is supported by means of n_s flexible supports (sup $i|_{i=1,\ldots,n_s}$). The movement of the crane's selected links is done by means of n_{dr} flexible drives (dr$p|_{p=2,\ldots,n_{dr}}$) with torque (force) $\mathbf{t}_{dr}^{(p)}$.

The motion of link p is described by the joint coordinates and defined by vector:

$$\mathbf{q}^{(p)}\Big|_{p=1,\ldots,n_l} = \left[\mathbf{q}^{(p-1)^T}\middle|\tilde{\mathbf{q}}^{(p)^T}\right]^T, \tag{1}$$

where $\mathbf{q}^{(0)} = \emptyset$.

The vector of generalized coordinates $\mathbf{q}^{(p)}$ contains

$$n_{dof}^{(p)}\Big|_{p=1,\ldots,n_l} = n_{dof}^{(p-1)} + \tilde{n}_{dof}^{(p)}, \tag{2}$$

components, where $n_{dof}^{(0)} = 0$.

The Denavit–Hartenberg notation is used to describe the geometry of particular links. The homogeneous transformation matrices from the local coordinate systems to the reference system {0} are determined according to the relationship:

$$\mathbf{T}^{(p)}\Big|_{p=1,\dots,n_l} = \mathbf{T}^{(p-1)}\tilde{\mathbf{T}}^{(p)}, \tag{3}$$

where $\mathbf{T}^{(0)} = \mathbf{I}$.

The equations of motion of the system are derived using the formalism of Lagrange equations:

$$\frac{\mathrm{d}}{\mathrm{d}t}\frac{\partial E_k}{\partial \dot{q}_j} - \frac{\partial E_k}{\partial q_j} + \frac{\partial E_p}{\partial q_j} + \frac{\partial R}{\partial \dot{q}_j} = 0,$$

where: $E_k = \sum_{p=1}^{n_l} E_k^{(p)}$,

$$E_p = E_{p,g} + E_{p,s} + E_{p,l} + E_{p,dr}^{(p)} = \sum_{p=1}^{n_l} E_{p,g}^{(p)} + \sum_{i=1}^{n_s} E_{p,s}^{(i)} + \sum_{p=1}^{n_f} E_{p,l}^{(p)} + \sum_{p=1}^{n_{dr}} E_{p,dr}^{(p)},$$

$$R = R_s + R_l + R_{dr} = \sum_{i=1}^{n_s} R_s^{(i)} + \sum_{p=1}^{n_f} R_l^{(p)} + \sum_{p=1}^{n_{dr}} R_{dr}^{(p)}.$$

However, this requires determination of the kinetic energy, potential energy (gravity forces, spring deformation), and the Rayleigh dissipation function of the system.

2.1. Kinetic energy and potential energy of gravity forces

The kinetic energy of link p is defined by the following formula:

$$E_k^{(p)} = \frac{1}{2}\mathrm{tr}\left\{\dot{\mathbf{T}}^{(p)}\mathbf{H}^{(p)}\dot{\mathbf{T}}^{(p)^T}\right\}, \tag{4}$$

where $\mathbf{H}^{(p)} = \begin{bmatrix} I_{(\hat{\mathbf{y}}^{(p)}\hat{\mathbf{z}}^{(p)})}^{(p)} & I_{\hat{\mathbf{x}}^{(p)}\hat{\mathbf{y}}^{(p)}}^{(p)} & I_{\hat{\mathbf{x}}^{(p)}\hat{\mathbf{z}}^{(p)}}^{(p)} & S_{\hat{\mathbf{x}}^{(p)}}^{(p)} \\ & I_{(\hat{\mathbf{x}}^{(p)}\hat{\mathbf{z}}^{(p)})}^{(p)} & I_{\hat{\mathbf{y}}^{(p)}\hat{\mathbf{z}}^{(p)}}^{(p)} & S_{\hat{\mathbf{y}}^{(p)}}^{(p)} \\ & & I_{(\hat{\mathbf{x}}^{(p)}\hat{\mathbf{y}}^{(p)})}^{(p)} & S_{\hat{\mathbf{z}}^{(p)}}^{(p)} \\ \text{sym.} & & & m^{(p)} \end{bmatrix}$,

$$I_{(\hat{\mathbf{y}}^{(p)}\hat{\mathbf{z}}^{(p)})}^{(p)} = \frac{1}{2}\left(-I_{\hat{\mathbf{x}}^{(p)}}^{(p)} + I_{\hat{\mathbf{y}}^{(p)}}^{(p)} + I_{\hat{\mathbf{z}}^{(p)}}^{(p)}\right), \quad I_{(\hat{\mathbf{x}}^{(p)}\hat{\mathbf{z}}^{(p)})}^{(p)} = \frac{1}{2}\left(I_{\hat{\mathbf{x}}^{(p)}}^{(p)} - I_{\hat{\mathbf{y}}^{(p)}}^{(p)} + I_{\hat{\mathbf{z}}^{(p)}}^{(p)}\right), \quad I_{(\hat{\mathbf{x}}^{(p)}\hat{\mathbf{y}}^{(p)})}^{(p)} = \frac{1}{2}\left(I_{\hat{\mathbf{x}}^{(p)}}^{(p)} + I_{\hat{\mathbf{y}}^{(p)}}^{(p)} - I_{\hat{\mathbf{z}}^{(p)}}^{(p)}\right).$$

The Lagrange operators of link p can be written in the following form:

$$\frac{\mathrm{d}}{\mathrm{d}t}\frac{\partial E_k^{(p)}}{\partial \dot{q}_j^{(p)}} - \frac{\partial E_k^{(p)}}{\partial q_j^{(p)}} = \left[\begin{array}{ccccc|c} \tilde{\mathbf{A}}_{1,1}^{(p)} & \dots & \tilde{\mathbf{A}}_{1,j}^{(p)} & \dots & & \tilde{\mathbf{A}}_{1,p}^{(p)} \\ \vdots & \ddots & \vdots & \iddots & & \vdots \\ \tilde{\mathbf{A}}_{i,1}^{(p)} & \dots & \tilde{\mathbf{A}}_{i,j}^{(p)} & \dots & & \tilde{\mathbf{A}}_{i,p}^{(p)} \\ \vdots & \iddots & \vdots & \ddots & & \vdots \\ \hline \tilde{\mathbf{A}}_{p,1}^{(p)} & \dots & \tilde{\mathbf{A}}_{p,j}^{(p)} & \dots & & \tilde{\mathbf{A}}_{p,p}^{(p)} \end{array}\right] \left[\begin{array}{c} \ddot{\tilde{\mathbf{q}}}^{(1)} \\ \vdots \\ \ddot{\tilde{\mathbf{q}}}^{(j)} \\ \vdots \\ \hline \ddot{\tilde{\mathbf{q}}}^{(p)} \end{array}\right] + \left[\begin{array}{c} \tilde{\mathbf{h}}_1^{(p)} \\ \vdots \\ \tilde{\mathbf{h}}_i^{(p)} \\ \vdots \\ \hline \tilde{\mathbf{h}}_p^{(p)} \end{array}\right], \tag{5}$$

where

$$\tilde{\mathbf{A}}_{i,j}^{(p)}\Big|_{i,j=1,\dots,p} = \left(\tilde{a}_{n_{dof}^{(i-1)}+k,\,n_{dof}^{(j-1)}+l}^{(p)}\right)_{\substack{k=1,\dots,\tilde{n}_{dof}^{(i)} \\ l=1,\dots,\tilde{n}_{dof}^{(j)}}}, \quad \tilde{a}_{i,j}^{(p)} = \mathrm{tr}\left\{\mathbf{T}_i^{(p)}\mathbf{H}^{(p)}\mathbf{T}_j^{(p)^T}\right\},$$

$$\tilde{\mathbf{h}}_i^{(p)}\Big|_{i=1,\dots,p} = \left(\tilde{h}_{n_{dof}^{(i-1)}+k}^{(p)}\right)_{k=1,\dots,\tilde{n}_{dof}^{(p)}}, \quad \tilde{h}_i^{(p)} = \sum_{m=1}^{n_{dof}^{(p)}}\sum_{n=m}^{n_{dof}^{(p)}} \mathrm{tr}\left\{\mathbf{T}_i^{(p)}\mathbf{H}^{(p)}\mathbf{T}_{m,n}^{(p)^T}\right\}\dot{q}_m^{(p)}\dot{q}_n^{(p)},$$

$$\mathbf{T}_m^{(p)} = \frac{\partial \mathbf{T}^{(p)}}{\partial q_m^{(p)}}, \quad \mathbf{T}_{m,n}^{(p)} = \frac{\partial^2 \mathbf{T}^{(p)}}{\partial q_m^{(p)}\partial q_n^{(p)}}.$$

The potential energy of gravity forces of link p is defined as:

$$E_{p,g}^{(p)} = m^{(p)} g \mathbf{j}_3 \mathbf{T}^{(p)} \mathbf{r}_{C^{(p)}}^{(p)}, \tag{6}$$

where: $\mathbf{j}_3 = [0 \quad 0 \quad 1 \quad 0]$.

The derivatives of Eq. (5) take the form:

$$\frac{\partial E_{p,g}^{(p)}}{\partial \mathbf{q}^{(p)}} = \begin{bmatrix} \tilde{\mathbf{g}}_1^{(p)} \\ \vdots \\ \tilde{\mathbf{g}}_i^{(p)} \\ \vdots \\ \tilde{\mathbf{g}}_p^{(p)} \end{bmatrix}, \tag{7}$$

where $\tilde{\mathbf{g}}_i^{(p)}|_{i=1,\dots,p} = (\tilde{g}^{(p)}_{n_{dof}^{(i-1)}+k})_{k=1,\dots,\tilde{n}_{dof}^{(i)}}$, $\tilde{g}_i^{(p)} = m^{(p)} g \mathbf{j}_3 \mathbf{T}_i^{(p)} \mathbf{r}_{C^{(p)}}^{(p)}$.

When considering the system of n_l rigid links, the kinetic energy and potential energy of gravity forces can be written, respectively, as follows:

$$E_k = \sum_{p=1}^{n_l} E_k^{(p)}, \quad E_{p,g} = \sum_{p=1}^{n_l} E_{p,g}^{(p)}, \tag{8}$$

and the equations of motion of n_l links can be written as follows:

$$\mathbf{A}\ddot{\mathbf{q}} = \mathbf{e} \tag{9}$$

where: $\mathbf{A} = \begin{bmatrix} \mathbf{A}_{1,1} & \cdots & \mathbf{A}_{1,j} & \cdots & \mathbf{A}_{1,n_l} \\ \vdots & \ddots & \vdots & ⋰ & \vdots \\ \mathbf{A}_{i,1} & \cdots & \mathbf{A}_{i,j} & \cdots & \mathbf{A}_{i,n_l} \\ \vdots & ⋰ & \vdots & \ddots & \vdots \\ \mathbf{A}_{n_l,1} & \cdots & \mathbf{A}_{n_l,j} & \cdots & \mathbf{A}_{n_l,n_l} \end{bmatrix}$, $\mathbf{A}_{i,j} = \sum_{l=\max\{i,j\}}^{n_l} \tilde{\mathbf{A}}_{i,j}^{(l)}$, $\mathbf{e} = \begin{bmatrix} \mathbf{e}_1 \\ \vdots \\ \mathbf{e}_i \\ \vdots \\ \mathbf{e}_{n_l} \end{bmatrix}$, $\mathbf{e}_i = -\sum_{l=i}^{n_l} (\tilde{\mathbf{h}}_i^{(l)} + \tilde{\mathbf{g}}_i^{(l)})$.

2.2. Modelling flexibility of the links

As was mentioned before, the rigid finite element method in the modified formulation is used to discretise the flexible links. In this method, flexible link p is replaced by the system of rigid elements (rfe) interconnected by means of spring-damping elements (sde). The procedure of the discretization is done in two stages. The first stage, called the primary division, consists of dividing the beam of length $l^{(p)}$ into $n_{div}^{(p)}$ sections of equal length $d^{(p)}$. The spring-damping features of the link are concentrated in $n_{sde}^{(p)}$ spring-damping elements and placed in the middle of each segment $d^{(p)}$ – Fig. 2a. In the second stage, called the secondary division (Fig. 2b), adjacent sections are connected into non-deformable rigid elements of acquiring characteristics inertia link. As a result of this discretization we obtain a system consisting of $n_{rfe}^{(p)}$ rigid finite elements ($n_{rfe}^{(p)} = n_{div}^{(p)} + 1$) of length

$$l^{(p,i)} = \begin{cases} d^{(p)}\big|_{i=1,\dots,n_{rfe}^{(p)}-2}, \\ \frac{1}{2} d^{(p)}\big|_{i\in\{0,n_{rfe}^{(p)}-1\}}, \end{cases} \tag{10}$$

which are interconnected by means of $n_{sde}^{(p)}$ spring-damping elements ($n_{sde}^{(p)} = n_{div}^{(p)}$).

The vector of generalized coordinates describing the motion of rfe $(p,i)\big|_{i=1,\dots,n_{rfe}^{(p)}}$ with respect to rfe $(p,i-1)$ has the form:

$$\tilde{\mathbf{q}}^{(p,i)} = \left(\tilde{q}_j^{(p,i)}\right)_{\substack{p=1,\dots,n_l \\ i=1,\dots,n_{rfe}^{(p)} \\ j=1,2,3}} = \begin{bmatrix} \psi^{(p,i)} & \theta^{(p,i)} & \varphi^{(p,i)} \end{bmatrix}^T. \tag{11}$$

Angles $\psi^{(p,\,i)}$ and $\theta^{(p,\,i)}$ correspond to the bending of link p in planes $\hat{\mathbf{x}}^{(p,i)}\hat{\mathbf{y}}^{(p,i)}$ and $\hat{\mathbf{x}}^{(p,i)}\hat{\mathbf{z}}^{(p,i)}$, respectively, whereas $\varphi^{(p,\,i)}$ is the angle of twist – Fig. 3.

The vector of generalized coordinates describing the motion of rfe $(p,\,i)$ with respect to reference system {0} has the following components:

$$\mathbf{q}^{(p,i)} = \left[\mathbf{q}^{(p-1)^T} \middle| \tilde{\mathbf{q}}^{(p,0)^T} \quad \tilde{\mathbf{q}}^{(p,i)^T} \right]^T. \tag{12}$$

The homogeneous transformation matrices from the local coordinates system of rfe $(p,\,i)$ to reference system {0} can be written as follows:

$$\mathbf{T}^{(p,i)} = \mathbf{T}^{(p,i-1)} \tilde{\mathbf{T}}^{(p,i)}. \tag{13}$$

This means that the flexible link is treated as a system of consecutive rigid elements (rfe), each having three-degrees-of-freedom in relative motion. Both the kinetic energy and the potential energy of the gravity forces are calculated according to

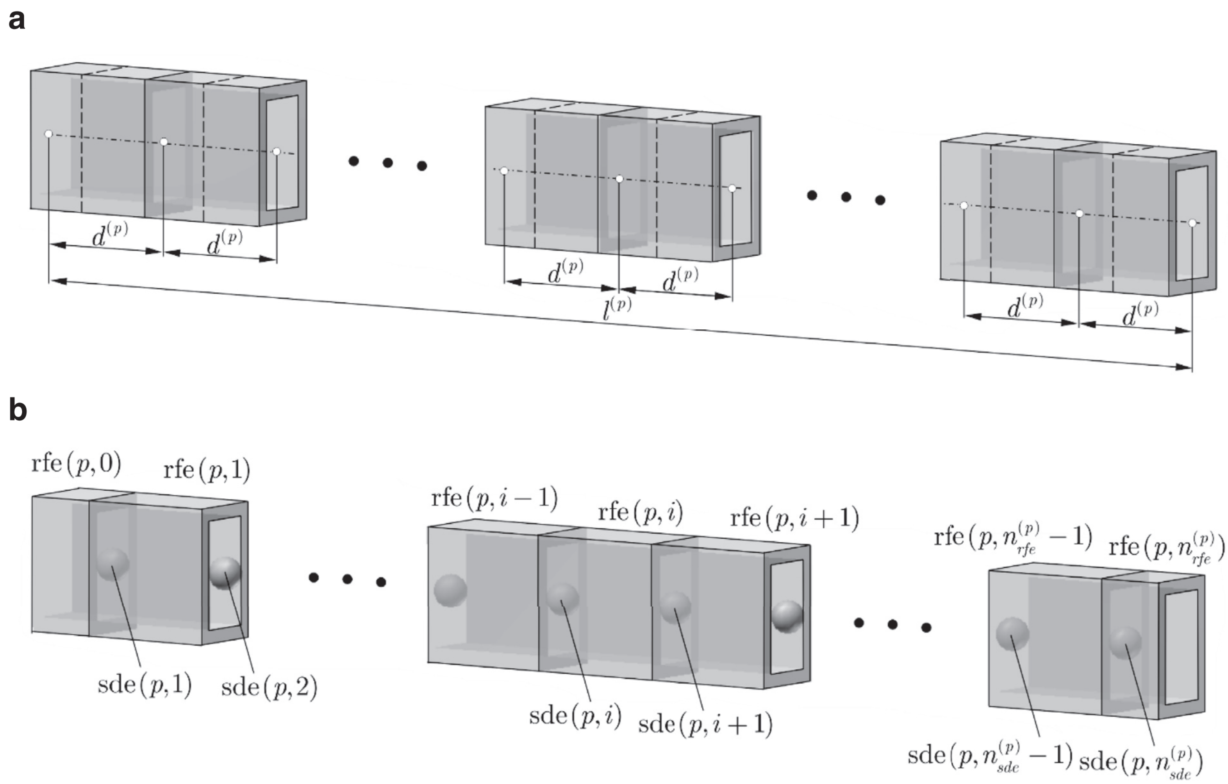

Fig. 2. Discretization of flexible link p: a) primary division b) secondary division.

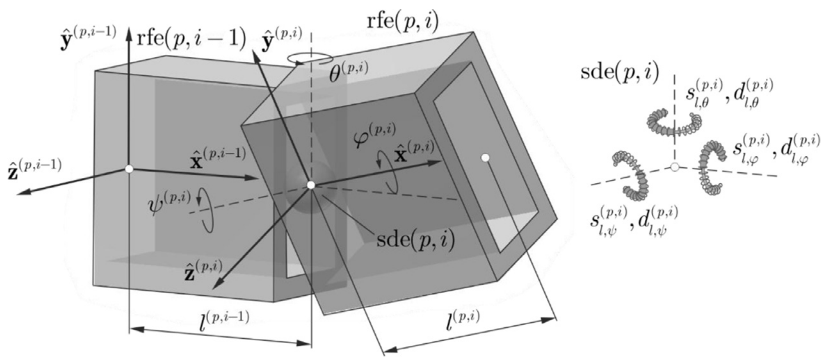

Fig. 3. Generalized coordinates rfe $(p,\ i)$.

the formulas that were outlined earlier. However, we need to take into account the potential energy of spring deformation and the Rayleigh dissipation function of link p, both of which are expressed by the relations:

$$E_{p,l}^{(p)} = \frac{1}{2}\sum_{i=1}^{n_{rfe}^{(p)}} \tilde{\mathbf{q}}^{(p,i)^T}\mathbf{S}_l^{(p,i)}\tilde{\mathbf{q}}^{(p,i)}, \quad R_l^{(p)} = \frac{1}{2}\sum_{i=1}^{n_{rfe}^{(p)}} \dot{\tilde{\mathbf{q}}}^{(p,i)^T}\mathbf{D}_l^{(p,i)}\dot{\tilde{\mathbf{q}}}^{(p,i)}, \tag{14}$$

where: $\mathbf{S}_l^{(p,i)} = \text{diag}\{s_{l,\psi}^{(p,i)}, s_{l,\theta}^{(p,i)}, s_{l,\varphi}^{(p,i)}\}$, $\mathbf{D}_l^{(p,i)} = \text{diag}\{d_{l,\psi}^{(p,i)}, d_{l,\theta}^{(p,i)}, d_{l,\varphi}^{(p,i)}\}$.

The derivatives of Eq. (14) take the form:

$$\frac{\partial E_{p,l}^{(p)}}{\partial \tilde{\mathbf{q}}^{(p,i)}} = \mathbf{S}_l^{(p)}\tilde{\mathbf{q}}^{(p,i)}, \quad \frac{\partial R_l^{(p)}}{\partial \dot{\tilde{\mathbf{q}}}^{(p,i)}} = \mathbf{D}_l^{(p)}\dot{\tilde{\mathbf{q}}}^{(p,i)}, \tag{15}$$

where: $\mathbf{S}_l^{(p)} = \text{diag}\{\mathbf{S}_l^{(p,1)}, \dots, \mathbf{S}_l^{(p,n_{rfe}^{(p)})}\}$, $\mathbf{D}_l^{(p)} = \text{diag}\{\mathbf{D}_l^{(p,1)}, \dots, \mathbf{D}_l^{(p,n_{rfe}^{(p)})}\}$.

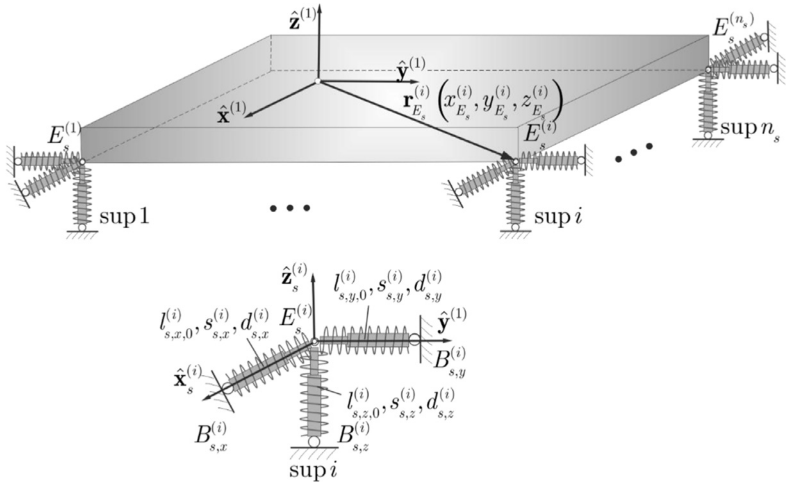

Fig. 4. Model of flexible supports.

2.3. Modeling of the flexibility of the supports

The forest crane is supported by means of n_s flexible supports ($\sup i|_{i=1,\dots,n_s}$), which are modeled using spring-damping elements – Fig. 4.

The potential energy of spring deformation and the Rayleigh dissipation function of $\sup i$ in α direction ($\alpha \in \{x, y, z\}$) can be defined as:

$$E_{p,s,\alpha}^{(i)} = \frac{1}{2} s_{s,\alpha}^{(i)} \left(e_{s,\alpha}^{(i)}\right)^2, \quad R_{s,\alpha}^{(i)} = \frac{1}{2} d_{s,\alpha}^{(i)} \left(\dot{e}_{s,\alpha}^{(i)}\right)^2, \tag{16}$$

where: $e_{s,\alpha}^{(i)} = l_{s,\alpha}^{(i)} - l_{s,\alpha,0}^{(i)}$,

$$l_{s,\alpha}^{(i)} = \left|\mathbf{U}_{E_s}^{(i)} \tilde{\mathbf{q}}^{(1)}\right|,$$

$$\mathbf{U}_{E_s}^{(i)} = \begin{bmatrix} 1 & 0 & 0 & | & 0 & z_{E_s}^{(i)} & -y_{E_s}^{(i)} \\ 0 & 1 & 0 & | & -z_{E_s}^{(i)} & 0 & x_{E_s}^{(i)} \\ 0 & 0 & 1 & | & y_{E_s}^{(i)} & -x_{E_s}^{(i)} & 0 \end{bmatrix}.$$

Generalizing, for any number of supports it can be written as:

$$E_{p,s} = \sum_{i=1}^{n_s} \sum_{\alpha \in \{x,y,z\}} E_{p,s,\alpha}^{(i)}, \quad R_s = \sum_{i=1}^{n_s} \sum_{\alpha \in \{x,y,z\}} R_{s,\alpha}^{(i)}. \tag{17}$$

The derivatives of Eq. (17) take the form:

$$\frac{\partial E_{p,s}}{\partial \tilde{\mathbf{q}}^{(1)}} = \sum_{i=1}^{n_s} \sum_{\alpha \in \{x,y,z\}} s_{s,\alpha}^{(i)} \left(l_{s,\alpha}^{(i)} - l_{s,\alpha,0}^{(i)}\right) \frac{1}{l_{s,\alpha}^{(i)}} \mathbf{U}_{E_s}^{(i)^T} \mathbf{U}_{E_s}^{(i)} \tilde{\mathbf{q}}^{(1)}, \quad \frac{\partial R_s}{\partial \dot{\tilde{\mathbf{q}}}^{(1)}} = \sum_{i=1}^{n_s} \sum_{\alpha \in \{x,y,z\}} d_{s,\alpha}^{(i)} \mathbf{U}_{E_s}^{(i)^T} \mathbf{U}_{E_s}^{(i)} \dot{\tilde{\mathbf{q}}}^{(1)}. \tag{18}$$

2.4. Modeling of flexibility of the drives

The selected links of the forest crane are driven using n_{dr} flexible drives ($\mathrm{dr}\, p|_{p=2,\dots,n_{dr}}$). The models of flexible drives with torque (force) $t_{dr}^{(p)}$ for revolute and prismatic joints are presented in Fig. 5a and 5b. The displacement $q_{dr}^{(p)}$ of the end of the dimensionless spring which models the flexibility of the drive varies according to the assumed function of time (Fig. 5c). Generalized coordinate $q_j^{(p)}$, which is an unknown quantity, is determined when solving the equations of motion.

The energy of spring deformation and the Rayleigh dissipation function of the drive can be expressed as follows:

$$E_{p,dr}^{(p)} = \frac{1}{2} s_{dr}^{(p)} \left(q_{dr}^{(p)} - q_j^{(p)}\right)^2, \quad R_{dr}^{(p)} = \frac{1}{2} d_{dr}^{(p)} \left(\dot{q}_{dr}^{(p)} - \dot{q}_j^{(p)}\right)^2. \tag{19}$$

The derivatives of Eq. (19) take the form:

$$\frac{\partial E_{p,dr}^{(p)}}{\partial q_j^{(p)}} = -s_{dr}^{(p)} \left(q_{dr}^{(p)} - q_j^{(p)}\right), \quad \frac{\partial R_{dr}^{(p)}}{\partial \dot{q}_j^{(p)}} = -d_{dr}^{(p)} \left(\dot{q}_{dr}^{(p)} - \dot{q}_j^{(p)}\right). \tag{20}$$

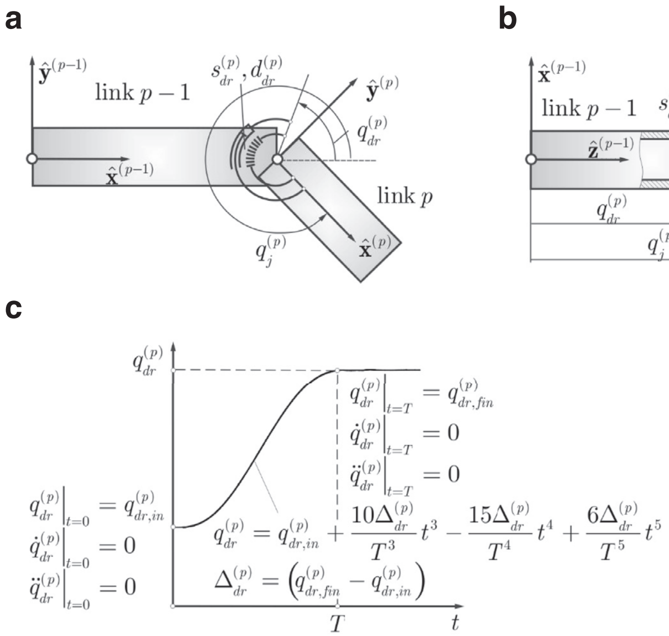

Fig. 5. Model of the flexible drive.

The driving torque (force) for the flexible drive in a revolute (prismatic) joint can be written in the following form:

$$t_{dr}^{(p)} = -\left(\frac{\partial E_{p,dr}^{(p)}}{\partial q_j^{(p)}} + \frac{\partial R_{dr}^{(p)}}{\partial \dot{q}_j^{(p)}}\right). \tag{21}$$

An example of the application of the models developed here will be presented based on a forest crane whose kinematic structure consists of eight links.

3. Example of analysis

The model of the forest crane analyzed here is presented in Fig. 6. It is assumed that only one link is treated as flexible. The crane is supported by means of eight flexible supports.

The generalized coordinates are the components of the vector:

$$\mathbf{q} = \left[\tilde{\mathbf{q}}^{(1)^T} \quad \tilde{\mathbf{q}}^{(2)^T} \quad \tilde{\mathbf{q}}^{(3,0)^T} \quad \tilde{\mathbf{q}}^{(3,i)^T} \quad \tilde{\mathbf{q}}^{(4)^T} \quad \tilde{\mathbf{q}}^{(5)^T} \quad \tilde{\mathbf{q}}^{(6)^T} \quad \tilde{\mathbf{q}}^{(7)^T} \quad \tilde{\mathbf{q}}^{(8)^T}\right]^T, \tag{22}$$

where: $\tilde{\mathbf{q}}^{(1)} = [x^{(1)} \quad y^{(1)} \quad z^{(1)} \quad \psi^{(1)} \quad \theta^{(1)} \quad \varphi^{(1)}]^T$, $\tilde{\mathbf{q}}^{(2)} = [\psi^{(2)}]$, $\tilde{\mathbf{q}}^{(3,0)} = [\psi^{(3)}]$, $\tilde{\mathbf{q}}^{(3,i)}|_{i=1,\dots,n_{rfe}^{(3)}} = [\psi^{(3,i)} \quad \theta^{(3,i)} \quad \varphi^{(3,i)}]^T$, $\tilde{\mathbf{q}}^{(4)} = [\psi^{(4)}]$, $\tilde{\mathbf{q}}^{(5)} = [z^{(5)}]$, $\tilde{\mathbf{q}}^{(6)} = [\psi^{(6)}]$, $\tilde{\mathbf{q}}^{(7)} = [\psi^{(7)}]$, $\tilde{\mathbf{q}}^{(8)} = [\psi^{(8)}]$.

The homogeneous transformation matrices have the following forms:

$$\tilde{\mathbf{T}}^{(1)} = \begin{bmatrix} c\psi^{(1)}c\theta^{(1)} & c\psi^{(1)}s\theta^{(1)}s\varphi^{(1)} - s\psi^{(1)}c\varphi^{(1)} & c\psi^{(1)}s\theta^{(1)}c\varphi^{(1)} + s\psi^{(1)}s\varphi^{(1)} & x^{(1)} \\ s\psi^{(1)}c\theta^{(1)} & s\psi^{(1)}s\theta^{(1)}s\varphi^{(1)} + c\psi^{(1)}c\varphi^{(1)} & s\psi^{(1)}s\theta^{(1)}c\varphi^{(1)} - c\psi^{(1)}s\varphi^{(1)} & y^{(1)} \\ -s\theta^{(1)} & c\theta^{(1)}s\varphi^{(1)} & c\theta^{(1)}c\varphi^{(1)} & z^{(1)} \\ 0 & 0 & 0 & 1 \end{bmatrix},$$

$$\tilde{\mathbf{T}}^{(2)} = \begin{bmatrix} c\psi^{(2)} & -s\psi^{(2)} & 0 & 0 \\ s\psi^{(2)} & c\psi^{(2)} & 0 & 0 \\ 0 & 0 & 1 & 0 \\ 0 & 0 & 0 & 1 \end{bmatrix}, \quad \tilde{\mathbf{T}}^{(3,0)} = \begin{bmatrix} c\psi^{(3)} & -s\psi^{(3)} & 0 & 0 \\ 0 & 0 & -1 & 0 \\ s\psi^{(3)} & c\psi^{(3)} & 0 & l^{(2)} \\ 0 & 0 & 0 & 1 \end{bmatrix},$$

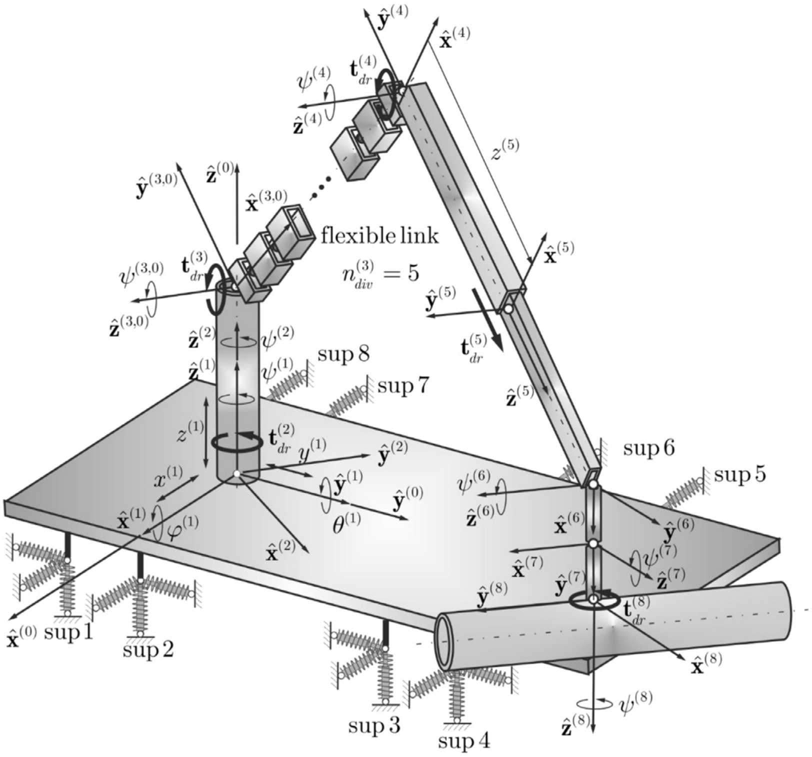

Fig. 6. Model of the forest crane.

$$\tilde{\mathbf{T}}^{(3,i)}\Big|_{i=1,\dots,n_{rfe}^{(p)}} = \begin{bmatrix} c\psi^{(3,i)}c\theta^{(3,i)} & c\psi^{(3,i)}s\theta^{(3,i)}s\varphi^{(3,i)} - s\psi^{(3,i)}c\varphi^{(3,i)} & c\psi^{(3,i)}s\theta^{(3,i)}c\varphi^{(3,i)} + s\psi^{(3,i)}s\varphi^{(3,i)} & l^{(3,i)} \\ s\psi^{(3,i)}c\theta^{(3,i)} & s\psi^{(3,i)}s\theta^{(3,i)}s\varphi^{(3,i)} + c\psi^{(3,i)}c\varphi^{(3,i)} & s\psi^{(3,i)}s\theta^{(3,i)}c\varphi^{(3,i)} - c\psi^{(3,i)}s\varphi^{(3,i)} & 0 \\ -s\theta^{(3,i)} & c\theta^{(3,i)}s\varphi^{(3,i)} & c\theta^{(3,i)}c\varphi^{(3,i)} & 0 \\ 0 & 0 & 0 & 1 \end{bmatrix},$$

$$\tilde{\mathbf{T}}^{(4)} = \begin{bmatrix} c\psi^{(4)} & -s\psi^{(4)} & 0 & l^{(3,n_{rfe}^{(3)})} \\ s\psi^{(4)} & c\psi^{(4)} & 0 & 0 \\ 0 & 0 & 1 & 0 \\ 0 & 0 & 0 & 1 \end{bmatrix}, \quad \tilde{\mathbf{T}}^{(5)} = \begin{bmatrix} 1 & 0 & 0 & 0 \\ 0 & 0 & -1 & -z^{(5)} \\ 0 & 1 & 0 & 0 \\ 0 & 0 & 0 & 1 \end{bmatrix},$$

$$\tilde{\mathbf{T}}^{(6)} = \begin{bmatrix} c\psi^{(6)} & -s\psi^{(6)} & 0 & 0 \\ 0 & 0 & 1 & 0 \\ -s\psi^{(6)} & -c\psi^{(6)} & 0 & 0 \\ 0 & 0 & 0 & 1 \end{bmatrix}, \quad \tilde{\mathbf{T}}^{(7)} = \begin{bmatrix} c\psi^{(7)} & -s\psi^{(7)} & 0 & l^{(6)} \\ 0 & 0 & 1 & 0 \\ -s\psi^{(7)} & -c\psi^{(7)} & 0 & 0 \\ 0 & 0 & 0 & 1 \end{bmatrix},$$

$$\tilde{\mathbf{T}}^{(8)} = \begin{bmatrix} c\psi^{(8)} & -s\psi^{(8)} & 0 & 0 \\ 0 & 0 & 1 & l^{(7)} \\ -s\psi^{(8)} & -c\psi^{(8)} & 0 & 0 \\ 0 & 0 & 0 & 1 \end{bmatrix}, \quad s\alpha^{(\beta)} = \sin\alpha^{(\beta)}, \;\; c\alpha^{(\beta)} = \cos\alpha^{(\beta)}.$$

The equations of motion of the forest crane can be written as follows:

$$\mathbf{A}\ddot{\mathbf{q}} = \mathbf{e} + \mathbf{f}_{s,l} + \mathbf{t}_{dr}, \tag{23}$$

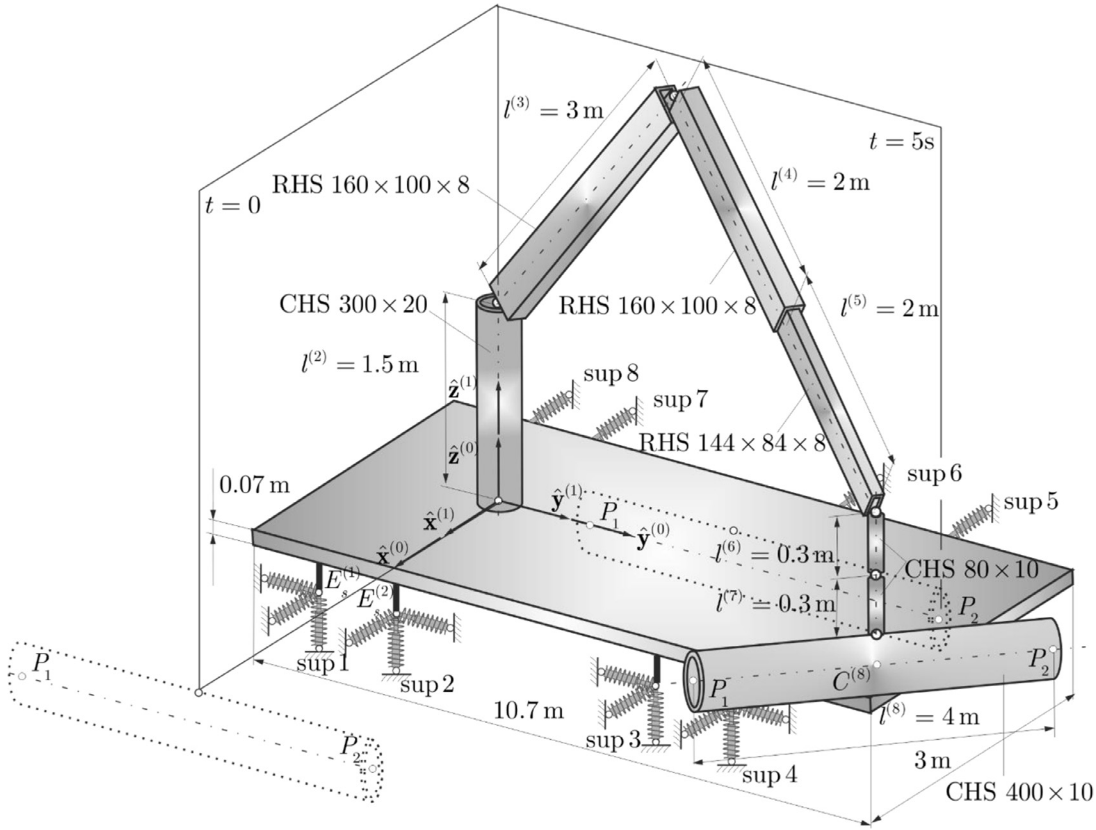

Fig. 7. Parameters and configuration of the system.

Table 1
Parameters of the supports.

sup i	1	2	3	4	5	6	7	8
$x_{E_s}^{(i)}$[m]	1.5	1.5	1.5	1.5	−1.5	−1.5	−1.5	−1.5
$y_{E_s}^{(i)}$[m]	0	1.0	8.0	9.0	9.0	8.0	1.0	0
$z_{E_s}^{(i)}$[m]					−0.57			
$l_{s,\alpha,0}^{(i)}\|_{\alpha\in\{x,y,z\}}$[m]					0			
$s_{s,\alpha}^{(i)}\|_{\alpha\in\{x,y\}}$[Nm^{-1}]					$3 \cdot 10^6$			
$s_{s,z}^{(i)}$[Nm^{-1}]					10^7			
$d_{s,\alpha}^{(i)}\|_{\alpha\in\{x,y\}}$[Nsm^{-1}]					$5 \cdot 10^4$			
$d_{s,z}^{(i)}$[Nsm^{-1}]					$9 \cdot 10^4$			

where **A, e** are defined by Eq. (8),

$$\mathbf{f}_{s,l} = \left[-\left(\frac{\partial E_{p,s}}{\partial \tilde{\mathbf{q}}^{(1)}} + \frac{\partial R_s}{\partial \dot{\tilde{\mathbf{q}}}^{(1)}} \right)^T \quad 0 \quad 0 \quad -\left(\frac{\partial E_{p,l}^{(3)}}{\partial \tilde{\mathbf{q}}^{(3,i)}} + \frac{\partial R_l^{(3)}}{\partial \dot{\tilde{\mathbf{q}}}^{(3,i)}} \right)^T \quad 0 \quad 0 \quad 0 \quad 0 \quad 0 \right]^T,$$

$$t_{dr} = \begin{bmatrix} 0 & t_{dr}^{(2)} & t_{dr}^{(3)} & 0 & t_{dr}^{(4)} & t_{dr}^{(5)} & 0 & 0 & t_{dr}^{(8)} \end{bmatrix}^T.$$

The equations of motion were integrated by using the classical explicit Runge–Kutta method of the fourth order with a constant step size equal to 10^{-4}s.

The geometrical parameters and initial and final configuration of the system analyzed here are presented in Fig. 7.

The parameters of the supports and drives are presented in Tables 1 and 2, respectively.

The influence of the flexibility of link 3 on the trajectories of selected points of load in $\hat{\mathbf{x}}^{(0)}\hat{\mathbf{y}}^{(0)}$ plane are presented in Fig. 8, whereas courses of the driving torques in the revolute joints and the driving force in the prismatic joint are shown in Fig. 9.

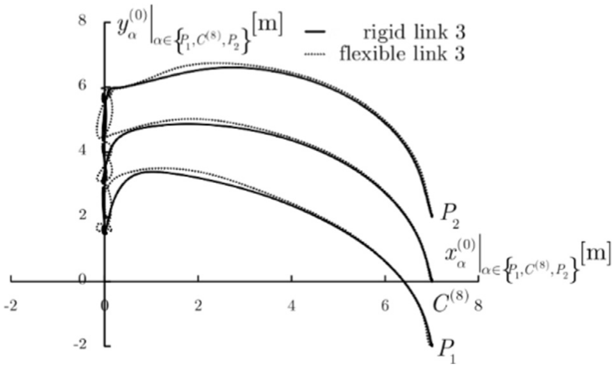

Fig. 8. Trajectories of selected points of the load.

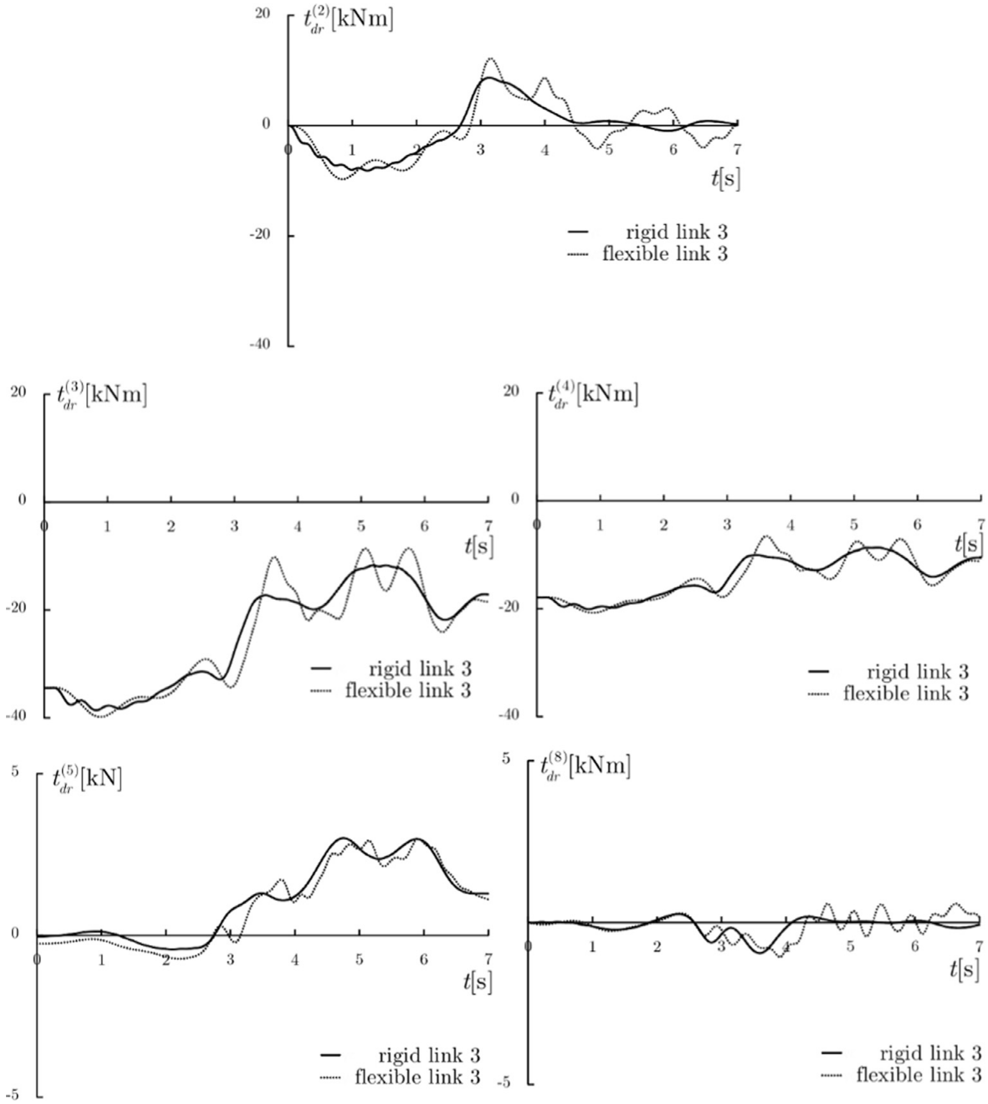

Fig. 9. Course of the driving torques and force.

Table 2
Parameters of the drives.

dr p	2	3	4	5	8
$q_{dr,in}^{(p)}$[rad], [m]	0	0	$\frac{1}{2}\pi$	2	$\frac{3}{2}\pi$
$q_{dr,fin}^{(p)}$[rad], [m]	$\frac{1}{2}\pi$	$\frac{7}{18}\pi$	$\frac{5}{18}\pi$	1	2π
$s_{dr}^{(p)}$[Nmrad^{-1}], [Nm^{-1}]	10^7	10^7	10^7	10^8	10^7
$d_{dr}^{(p)}$[Nsmrad^{-1}], [Nsm^{-1}]	$7 \cdot 10^3$	$7 \cdot 10^3$	$7 \cdot 10^3$	$6 \cdot 10^4$	$7 \cdot 10^3$

Analyzing the plots, there is a significant influence of flexibility of link 3 on load motion, and significant oscillations in the final phase of the movement can be observed. In the case of the courses of the driving torques in the revolute joints and the driving force in the prismatic joint, flexibility of the link causes a significant increase in their value.

4. Conclusions

The general mathematical model of a forest crane for a statics and dynamics analysis is presented in the paper. The flexibility of the support system, links and drives is assumed in the model. The rigid finite element method is used to take into account the flexibility of the links. The model presented here can be treated as a virtual prototype and, by performing computer simulations, can significantly support the constructor in the design of the real prototype. The statics and dynamics analysis of the forest crane, which is built of eight links, is presented as an example of the model. The results of numerical calculations show a significant influence of the flexibility link on the behavior of the crane and can be useful in the strength analysis of its components, including load bearing, and also in the selection of the drive systems.

References

[1] J. Kłosiński, Swing-free stop control of the slewing motion of the mobile crane, Control Eng. Pract. 13 (2005) 451–460.
[2] A. Maczyński, Load positioning and minimization of load oscillations for rotary cranes, J. Theor. Appl. Mech. 41 (4) (2003) 873–885.
[3] A. Maczyński, S. Wojciech, Dynamics of a mobile crane and optimization of the slewing motion of its upper structure, Nonlinear Dyn. 32 (3) (2003) 410–417.
[4] B. Posiadała, Influence of crane support system on motion of the lifted load, Mech. Mach. Theory 32 (1) (1997) 9–20.
[5] B. Posiadała, Modeling and analysis of the dynamics of load carrying system, in: Proceedings of World Congress on Engineering and Computer Science, 2, San Francisco USA, 2012.
[6] W. Sochacki, The dynamic stability of a laboratory model of a truck crane, Thin-Walled Struct. 45 (2007) 927–930.
[7] Z. Towarek, The dynamic stability of a crane standing on soil during the rotation of the boom, Int. J. Mech. Sci. 40 (6) (1998) 557–574.
[8] Z. Towarek, The function of the rheological soil strain under the foot supporting the crane, Arch. Mech. Eng. 46 (1) (1999) 5–18.
[9] A. Urbaś, Application of the rigid finite element method in the dynamics of grab cranes, Dyn. Syst. –Math. Numer. Approaches 3 (2015) 555–566 Łódź.
[10] A. Urbaś, Analysis of flexibility of the support and its influence on dynamics of the grab crane, Latin Am. J. Solids Struct. 10 (1) (2013) 109–121.
[11] B. Jerman, P. Podrzaj, J. Kramar, An inestigation of slewing-crane dynamics during slewing motion – development and verification of a mathematical model, Int. J. Mech. Sci. 46 (2004) 729–750.
[12] B. Jerman, J. Kramar, Study of the horizontal inertial forces acting on the suspended load of slewing cranes, Int. J. Mech. Sci. 50 (2008) 490–500.
[13] S. Kilicaslan, T. Balkan, S.K. Ider, Tipping load of mobile cranes with flexible booms, J. Sound Vib. 223 (4) (1999) 645–657.
[14] A. Trąbka, Influence of flexibilities of cranes structural components on load trajectory, J. Mech. Sci. Technol. 30 (1) (2016) 1–14.
[15] A. Trąbka, Dynamics of telescopic cranes with flexible structural components, Int. J. Mech. Sci. 88 (2014) 162–174.
[16] R.M. Ghigliazza, P. Holmes, On the dynamics of crane, or spherical pendula with moving supports, Int. J. Non-Linear Mech. 37 (2002) 1211–1221.
[17] K. Tanizumi, T. Yoshimura, J. Hino, T. Sakai, Modelling of dynamic behaviour and control of truck cranes, Trans. Jpn. Soc. Mech. Eng. 61 540-556 4629–4637.
[18] G. Sun, M. Kleeberger, Dynamic response of hydraulic mobile crane with consideration of the drive system, Mech. Mach. Theory 38 (2003) 1489–1508.
[19] T. Yoshimoto, Y. Sakawa, Modeling and control of a rotary crane with a flexible joint, Opt. Control Appl. Methods 10 (1989) 21–38.
[20] E. Papadopoulos, S. Sarkar, On the dynamic modeling of an articulated electrohydraulic forestry machine,, in: Proceedings of the 1996 AIAA Forum on Advanced Developments in Space Robotics, WI, 1996 1-2 August.
[21] E. Papadopoulos, R. Frenette, B. Mu, Y. Gonthier, On the modeling and control of an experimental harvester machine manipulator, in: Proceedings of IEEE/RSJ International Conference on Intelligent Robots and Systems, Grenoble, France, 1997, pp. 8–12.
[22] A. Urbaś, Dynamic Analysis and Control of Flexible Supported Machines, University of Bielsko-Biala, Bielsko-Biala, 2011 PhD. Thesis (in Polish).
[23] B. Posiadała, P. Waryś, D. Cekus, M. Tomala, The dynamics of the forest crane during the load carrying, Int. J. Struct. Stab. Dyn. 13 (7) (2013), doi:10.1142/S0219455413400130.
[24] P. La Hera, D.O. Morales, Non-linear dynamics modelling description for simulating the behavior of forestry cranes, Int. J. Model. Identif. Control 21 (2) (2014) 125–138.
[25] D.O. Morales, S. Westerberg, P.X. La Hera, U. Mettin, L. Freidovich, A.S. Shiriaev, Increasing the level of automation in the forestry logging process with crane trajectory planning and control, J. Field Robot. 31 (3) (2014) 343–363.
[26] P. La Hera, D.O. Morales, Model-based development of control systems for forestry cranes, J. Control Sci. Eng. vol. 2015 (2015) Article ID 256951, 15 pages, doi:10.1155/2015/256951.
[27] J. Kruszewski, W. Gawroński, E. Wittbrodt, F. Najbar, S. Grabowski, The Rigid Finite Element Method, Arkady Press, Warsaw, 1975 (in Polish).
[28] J. Kruszewski, S. Sawiak, E. Wittbrodt, The Rigid Finite Element Method in Dynamics, Science and Technical Publishers, Warsaw, 1999 (in Polish).
[29] T. Kawai, K. Kondou, New beam and plate bending elements in finite element analysis, J. Seisan Kenkyu 1 (1976) 27–30.
[30] T. Kawai, Some consideration on the finite element method, Int. J. Numer. Methods Eng. 16 (1980) 81–120.
[31] S. Wojciech, in: The dynamics of plane link mechanisms with the flexibility of links and the friction as well as the clearance in the joints, 463, Łódź University of Technology Press, 1984.
[32] A. Adamiec-Wójcik, Modelling Dynamics of Multibody Systems Using Homogeneous Transformations, 3, Bielsko-Biała University Press, 2003 Bielsko-Biała.
[33] J. Denavit, R.S. Hartenberg, A kinematic notation for lower-pair mechanisms based on matrices, J. Appl. Mech., 23, 215–221
[34] J.J. Craig, Introduction to Robotics. Mechanics and Control, Addison-Wesley Publishing Company, Inc., 1989.

[35] G. Legnani, F. Casalo, P. Righettini, B. Zappa, A homogeneous matrix approach to 3D kinematics and dynamics – I. Theory, Mech. Mach. Theory 31 (5) (1996) 586–605.
[36] G. Legnani, F. Casalo, P. Righettini, B. Zappa, A homogeneous matrix approach to 3D kinematics and dynamics – II. Applications to chains of rigid bodies and serial manipulators, Mech. Mach. Theory 31 (5) (1996) 573–587.
[37] E.I. Jurevič (Ed.), Dynamics of Robot Control Nauka, Moscow, 1984 (in Russian).
[38] E. Wittbrodt, I. Adamiec-Wójcik, S. Wojciech, Dynamics of flexible multibody systems, Rigid Finite Element Method, Springer, Berlin-Heidelberg, 2006.